Chapter 4

Assessment of Mitochondrial Dysfunction in Lymphocytes of Patients with Systemic Lupus Erythematosus

Andras Perl, Robert Hanczko, and Edward Doherty

Abstract

Systemic lupus erythematosus (SLE) is characterized by abnormal activation and cell death signaling within the immune system. Activation, proliferation, or death of cells of the immune system is dependent on controlled reactive oxygen intermediates (ROI) production and ATP synthesis in mitochondria. The mitochondrial transmembrane potential ($\Delta\psi_m$) reflects the energy stored in the electrochemical gradient across the inner mitochondrial membrane which, in turn, is used by F_0F_1-ATPase to convert ADP to ATP during oxidative phosphorylation. Mitochondrial hyperpolarization (MHP) and transient ATP depletion represent early and reversible steps in T cell activation and apoptosis. By contrast, T lymphocytes of patients with SLE exhibit elevated $\Delta\psi_m$, i.e., persistent mitochondrial hyperpolarization (MHP), cytoplasmic alkalinization, increased ROI production, as well as diminished levels of intracellular glutathione and ATP. Increased production of nitric oxide has been identified as a cause of MHP and increased mitochondrial biogenesis. Oxidative stress affects signaling through the T cell receptor as well as activity of redox-sensitive caspases. ATP depletion causes diminished activation-induced apoptosis and sensitizes lupus T cells to necrosis. Activation of the mammalian target of rapamycin (mTOR) has recently emerged as a key sensor of MHP and mediator of enhanced Ca^{2+} flux in lupus T cells.

Key words: Systemic lupus erythematosus, Mitochondrial hyperpolarization, Reactive oxygen intermediates, Cytoplasmic alkalinization, Caspases, Glutathione depletion, ATP depletion, Apoptosis, Necrosis, mTOR

1. Introduction

Systemic lupus erythematosus (SLE) is a chronic inflammatory disease characterized by T and B cell dysfunction and production of antinuclear antibodies. Abnormal T cell activation and cell death underlie the pathology of SLE (1, 2). Potentially autoreactive T and B lymphocytes during development (3) and after completion

Andras Perl (ed.), *Autoimmunity: Methods and Protocols*, Methods in Molecular Biology, vol. 900,
DOI 10.1007/978-1-60761-720-4_4,

of an immune response are removed by apoptosis (4). Paradoxically, lupus T cells exhibit both enhanced spontaneous apoptosis and defective activation-induced cell death. Increased spontaneous apoptosis of peripheral blood lymphocytes (PBL) has been linked to chronic lymphopenia (5) and compartmentalized release of nuclear autoantigens in patients with SLE (6). By contrast, defective CD3-mediated cell death may be responsible for persistence of autoreactive cells (7).

1.1. Mitochondrial Checkpoints of T Cell Activation and Apoptosis

Both cell proliferation and apoptosis are energy-dependent processes. Energy in the form of ATP is provided through glycolysis and oxidative phosphorylation. The mitochondrion, the site of oxidative phosphorylation, has long been identified as a source of energy and cell survival (8). The synthesis of ATP is driven by an electrochemical gradient across the inner mitochondrial membrane maintained by an electron transport chain and the membrane potential (negative inside and positive outside). A small fraction of electrons react directly with oxygen and form reactive oxygen intermediates (ROI). Disruption of the mitochondrial membrane potential has been proposed as the point of no return in apoptotic signaling (9–11). Mitochondrial membrane permeability is subject to regulation by an oxidation–reduction equilibrium of ROI, pyridine nucleotides (NADH/NAD + NADPH/NADP) and GSH levels (12). Regeneration of GSH by glutathione reductase from its oxidized form, GSSG, depends on NADPH produced by the pentose phosphate pathway (PPP) (13). ROI levels and $\Delta\psi_m$ are regulated by the supply of reducing equivalents from PPP (14, 15). While ROI have been considered as toxic by-products of aerobic existence, evidence is now accumulating that controlled levels of ROI modulate various aspects of cellular function and are necessary for signal-transduction pathways, including those mediating T cell activation and apoptosis (16).

Increased production of ROI was demonstrated in TNF (17–19) and Fas-mediated cell death (9, 14, 20–23). Disruption of the mitochondrial membrane potential ($\Delta\psi_m$) has been proposed as the point of no return in apoptotic signaling (9–11). Interestingly, elevation of $\Delta\psi_m$, mitochondrial hyperpolarization (MHP), and ROI production precede phosphatidylserine (PS) externalization and a disruption of $\Delta\psi_m$ in Fas- (15) and H_2O_2-induced apoptosis of Jurkat human leukemia T cells and normal human peripheral blood lymphocytes (24). These observations were extended to p53 (25), tumor necrosis factor α (26), staurosporin (27), camptothecin (28), and nitric oxide-induced apoptosis (29). Elevation of $\Delta\psi_m$ is independent from activation of caspases and represents an early event in apoptosis (15, 25). Pretreatment with caspase inhibitors, DEVD, Z-VAD, and Boc-Asp, completely abrogated Fas-induced PS externalization, indicating that activation of caspase-3, caspase-8,

and related cysteine proteases were absolutely required for cell death (30–33). ROI levels were partially inhibited in DEVD-treated Jurkat cells, suggesting that caspase-3 activation, perhaps through damage of mitochondrial membrane integrity, contributes to ROI production and serves as a positive feedback loop at later stages of the apoptotic process. Nevertheless, ROI levels remained significantly elevated after pretreatment with caspase inhibitors. This suggested that activation of caspase-3 or caspase-8 was not required for increased ROI production and $\Delta\psi_m$ hyperpolarization. By contrast, DEVD, Z-VAD, and Boc-Asp blocked PS externalization and decline of $\Delta\psi_m$ in annexin V-positive Jurkat cells, suggesting that disruption of $\Delta\psi_m$ (1) was a relatively late event with respect to ROI production and $\Delta\psi_m$ hyperpolarization and (2) depended on activation of caspase-3 and related proteases. The precise mechanism by which Fas and TNF signaling leads to changes in $\Delta\psi_m$ and ROI levels remains to be defined. Cleavage of cytosolic bid by caspase-8 generates a p15 carboxyterminal fragment that translocates to mitochondria. This may represent the initial insult to mitochondria in the Fas/TNF pathway (34).

MHP appears to be the earliest change associated with Fas (15), H_2O_2 (24), HIV-1 (35), p53 (25), TNFα (26), staurosporin (27), camptothecin (28), and NO-induced apoptosis (29). Elevation of $\Delta\psi_m$ is also triggered by activation of the CD3/CD28 complex (36) or stimulation with Con A (15), IL-10, IL-3, IFN-γ, or TGFβ (37). Therefore, elevation of $\Delta\psi_m$ or MHP represents an early but reversible switch not exclusively associated with apoptosis. With $\Delta\psi_m$ hyperpolarization and extrusion of H+ ions from the mitochondrial matrix, the cytochromes within the electron transport chain become more reduced which favors generation of ROI (38). MHP is caused by exposure to nitric oxide (NO) which is produced during T cell activation (39). Reduced glutathione (GSH) is profoundly depleted in lymphocytes of SLE patients (36) (Table 1), which may predispose to persistent MHP via *S*-nitrosylation of complex I upon exposure to NO (40). Thus, the effect of NO on MHP is tightly related to GSH levels. With MHP and extrusion of H+ ions from the mitochondrial matrix, the cytochromes within the electron transport chain become more reduced which promotes ROI production and generates oxidative stress (8). Diminished production of GSH in face of MHP and increased ROI production are suggestive of a severe metabolic defect in lupus T cells. The activation of the mammalian target of rapamycin (mTOR) has recently emerged as a key sensor of MHP (41) and mediator of enhanced Ca^{2+} flux in lupus T cells (42). mTOR activation may influence Ca^{2+} flux through interaction with HRES-1/Rab4, a regulator of endocytic recycling of CD3 and CD4 (Fig. 1) (43).

1.2. Pharmacological Targeting of Mitochondrial Dysfunction in SLE

MHP predisposes for increased ROI production (38). Oxidative stress affects activity of transcription factors AP-1 and NF-κB (44, 45), and, further downstream, may lead to the skewed expression of IL-2, TNF, and IL-10 (46). Increased spontaneous apoptosis of lymphocytes has been linked to increased IL-10 production, release of Fas ligand, and overexpression of Fas receptor in SLE (47). Since increased ROI levels confer sensitivity to H_2O_2, NO, TNF, and Fas-induced cell death (14, 15), elevated baseline

Table 1
Signaling abnormalities of T cell death in patients with SLE

Signal	Effect	Reference
$\Delta\psi_m$ ↑	ROI ↑, ATP ↓	(36)
ROI ↑	Spontaneous apoptosis ↑, IL-10 production ↑	(36, 37)
GSH ↓	ROI ↑, Spontaneous apoptosis ↑	(14, 36)
Spontaneous apoptosis ↑	Compartmentalized autoantigen release, disease activity ↑	(5, 6, 36, 76)
H_2O_2	Apoptosis ↓, necrosis ↑	(36)
CD3/CD28	AICD ↓, necrosis ↑	(37)
ATP ↓	Predisposes for necrosis	(36, 64)
Necrosis ↑	Inflammation ↑	(36), (77)
AICD ↓	Persistence of autoreactive cells	(7, 37)
FasR ↑	Spontaneous apoptosis ↑	(76)
FasL ↑	Spontaneous apoptosis ↑	(47)
IL-10 ↑	Selective induction of apoptosis in SLE	(37, 47, 78)
NO ↑	MHP, mTOR ↑	(39, 43, 50)
IL-10 blockade	Spontaneous apoptosis ↓, ROI ↓	(37, 47)
IL-12	Spontaneous apoptosis ↓, ROI ↓	(37)

↑: increase; ↓: decrease

Fig. 1. (continued) space (34). Phosphorylation of BAD by mitochondria-anchored PKA results in anti-apoptotic sequestration of BAD into the cytosol (85). Signaling through cell death receptors, such as Fas (15), CD3/CD28 co-stimulation (36, 37), ROS (24), NO (29), as well as lymphokines, IL-3, IL-10, IFN-γ, and TGF-β_1 influence $\Delta\psi_m$, ATP synthesis and susceptibility to apoptosis (37). MHP and mitochondrial biogenesis is mediated via production of NO by eNOS or nNOS (39) and up-regulation of transcription factors PGC-1α, Tfam, and ALAS (86). NO production by eNOS may be compartmentalized to the T cell synapse (87). NO causes transient MHP via reversible inhibition of complex IV/cytochrome c oxidase (29) and persistent MHP via *S*-nitrosylation of complex I of the ETC in a state of GSH depletion (40). mTOR senses $\Delta\psi_m$ (41), interacts with the small GTPase HRES-1/Rab4 (43), and regulates Ca^{2+} release (42).

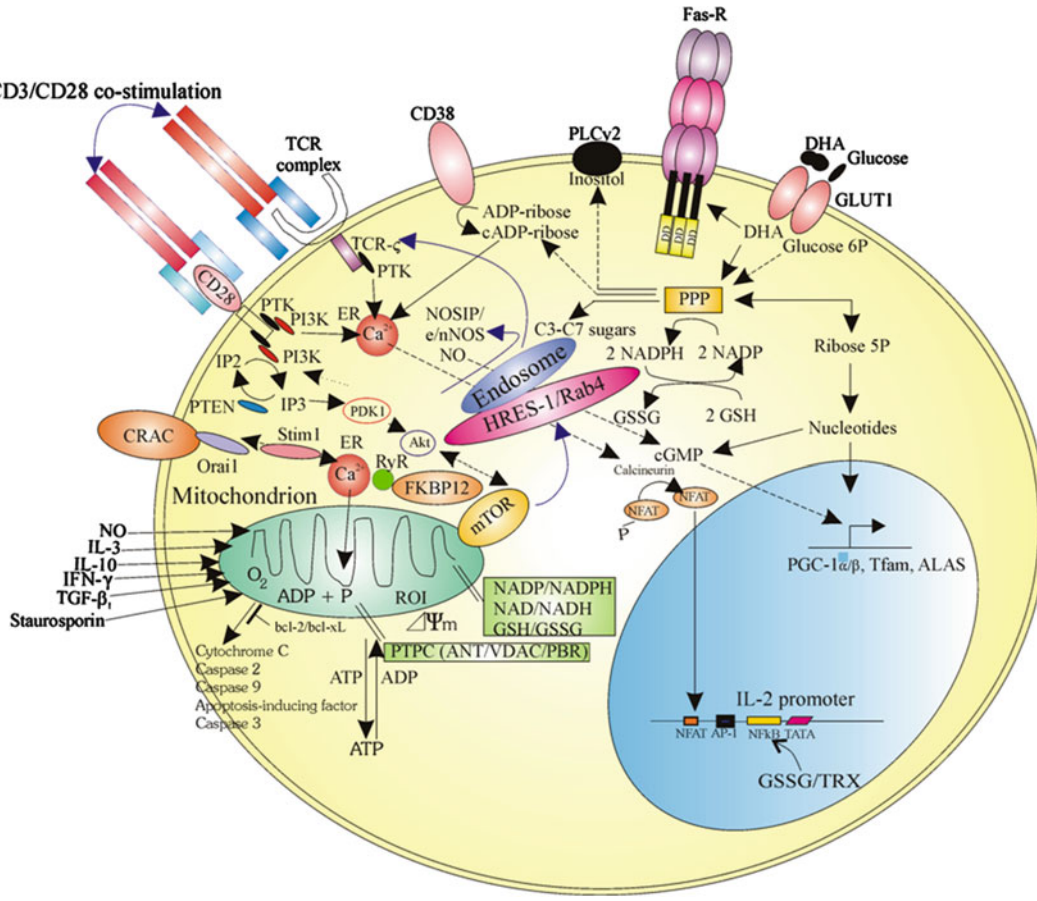

Fig. 1. Overview of mitochondrial redox and metabolic checkpoints of T cell activation and apoptosis signals. Antigen binding-initiated signaling through the T cell receptor complex/CD3 and the CD28 co-stimulatory molecule activate phsophatidylinositol 3-kinase (PI3K) and protein tyrosine kinases (PTK). Increased cytosolic Ca^{2+} concentration activates the serine/threonine phosphatase calcineurin which dephosphorylates the NFAT. Dephosphorylated NFAT can translocate to the nucleus where it promotes transcription of IL-2 in concert with AP-1, NF6B, and Oct-1. Ca^{2+} flux into mitochondria increases production of ROS and NF-6B activation (79–81). Mitochondrial membrane integrity is maintained by a balance of membrane-stabilizing bcl-2 and bcl-X_L and pore-inducing bax and bad (34) as well as the metabolic capacity to synthesize reducing equivalents, NADPH, GSH, and TRX. Controlled increase of ROS levels activates NF-6B and promotes cell growth. Excess ROS production and disruption of Δy_m lead to activation-induced cell death executed by caspase 3 (digesting vitally important proteins PARP, 70K U1RNP, lamin, and actin) and caspase 3-dependent DNase (CAD, causing nuclear DNA fragmentation). Cleavage by caspase 3 is thought to expose cryptic epitomes and cause autoantigenicity of self antigens (82). Activity of redox-sensitive transcription factors NF-6B, p53, AP-1, and Sp1 is regulated through release from inhibitor complexes and conformational changes in their active sites. Intracellular antioxidants reduced glutathione (GSH) and thioredoxin (TRX-DT) are regenerated at the expense of NADPH supplied primarily through metabolism of glucose via the pentose phosphate pathway (PPP) (83). Among PPP products, ribose 5-phosphate is required for nucleotide and DNA synthesis and support cell growth, C3–C7 sugars influence mitochondrial function and ROS production, inositol and ADP-ribose serve as precursors for second messengers, inositol phosphates and cADP-ribose, respectively. Dehydroascorbate (DHA) is imported through GLUT1. DHA is metabolized through the PPP, thereby enhancing GSH levels. DHA also increases surface expression of Fas-R (84). Glutathione reductase and TRX reductase synthesize GSH and TRX-DT at the expense of NADPH. Formulation of the PPP and its efficiency to provide NADPH is dependent on the expression of G6PD and TAL (14, 15). Δy_m is controlled by intracellular GSH/NADH/NADPH levels, integrity of the permeability transition pore complex largely comprised of adenine nucleotide translocator (ANT, inner membrane), voltage-dependent anion channel (VDAC, outer membrane), and translocation and dimerization of pro- and anti-apoptotic bcl-2 family members in the intermembrane

$\Delta\psi_m$, ROI production, and pH_i may have key roles in altered activation and death of lupus T cells. Although MHP was not affected, IL-10 antibody or IL-12 normalized ROI production and intracellular alkalinization in lupus PBL (37). Therefore, IL-10 antagonists may partially correct signaling dysfunction in lupus.

Recent studies showed diminished GSH/GSSG ratios in the kidneys of 8-month-old vs. 4-month-old (NZB × NZW) F1 mice; treatment with *N*-acetylcysteine (NAC), a precursor of GSH and stimulator of its de novo biosynthesis, prevented the decline of GSH/GSSG ratios, reduced autoantibody production and development of glomerulopnephritis (GN) and prolonged the survival of (NZB × NZW) F1 mice (48). Oral NAC has been used to treat oxidative stress in patients with idiopathic pulmonary fibrosis (IPF) (49). In a 1-year study of IPF patients treated with prednisone and azathioprine, addition of NAC (3 × 600 mg/day) improved vital capacity and reduced myelotoxicity in comparison to placebo. Therefore, prospective clinical studies appear justified to assess whether NAC treatment can reverse GSH depletion, correct T cell signaling defects and provide clinical benefit to patients with lupus.

NO production is a particularly interesting target because it provides a link between seemingly dissociated features of T cell activation and mitochondrial function. NO induces MHP and mitochondrial biogenesis, increases Ca^{2+} in the cytosol and mitochondria of normal T cells, and recapitulates the enhanced CD3/CD28-induced Ca^{2+} fluxing of lupus T cells (50). NO contributes to the development of GN in the MRL/*lpr* lupus mouse model (51). Inactivation of iNOS does not block the development of lupus (52), suggesting a role for eNOS and nNOS isoforms expressed in T cells. However, given the widespread expression of these isoforms in vascular smooth muscle and brain, it will be necessary to develop T-cell-specific approaches for inhibiting NOS to avoid potentially deleterious side effects.

2. Materials

1. Ficoll-Paque Plus (Amersham-Pharmacia, Uppsala, Sweden).
2. RPMI 1640 medium, fetal calf serum, penicillin, streptomycin, amphotericin B (Life Technologies, Grand Island, NY).
3. OKT3 monoclonal antibody (CRL 8001 from ATCC, Rockville, MD).
4. CD28.2 monoclonal antibody (Pharmingen, San Diego, CA).
5. Cytokines: IL-2, IL-3, IL-4, IL-6, IL-7, IL-10, IL-12, IL-15, TNF-α, TGF-β_1, and IFN-γ (PeproTech, Rocky Hill, NJ).

6. Polyclonal goat anti-human IL-10 neutralizing antibody (R&D Systems, Minneapolis, MN).
7. Annexin binding buffer: 10 mM HEPES pH 7.4, 140 mM NaCl, and 2.5 mM $CaCl_2$.
8. Phosphate-buffered saline (PBS): 8 g of NaCl, 0.2 g of KCl, 1.44 g of Na_2HPO_4, 0.24 g of KH_2PO_4 dissolved in 1 l of H_2O with pH adjusted to 7.4.
9. Fluorescein-conjugated annexin V (annexin V-FITC) and phycoerythrin-conjugated annexin V (annexin V-PE, R & D Systems, Minneapolis, MN).
10. Propidium iodide (R&D Systems).
11. Triton X-100 (Sigma, St. Louis, MO).
12. Hydroethidine (HE, Molecular Probes, Eugene, OR).
13. Quantum Red/Cy5-conjugated monoclonal antibodies directed to CD3, CD4, CD8, CD14 (Sigma, St. Louis, MO), CD45RA, and CD45RO (Pharmingen, San Diego, CA).
14. Fluorescence microscope: Nikon Eclipse E800 camera (Nikon Corporation, Tokyo, Japan). Equipped with SPOT digital camera (Diagnostic Instruments, Sterling Heights, MI).
15. Flow cytometer: Becton Dickinson FACStar Plus flow cytometer equipped with an argon ion laser delivering 200 mW of power at 488 nm.
16. Oxidation-sensitive fluorescent probes 5,6-carboxy-2′,7′-dichlorofluorescein-diacetate (DCFH-DA), dihydrorhodamine 123 (DHR) and hydroethidine (HE, Molecular Probes, Eugene, OR).
17. Cationic lipophilic dyes with high binding affinity to mitochondria: 3,3′-dihexyloxacarbocyanine iodide ($DiOC_6$), 5,5′,6,6′-tetrachloro-1,1′,3,3′-tetraethylbenzimida zolocarbocyanine iodide (JC-1), tetramethylrhodamine, methyl ester, perchlorate (TMRM), all from Molecular Probes (Eugene, OR).
18. Carbonyl cyanide *m*-chlorophenylhydrazone (mClCCP, Sigma).
19. Luminometer: AutoLumat LB953 (Berthold GmbH, Wildbad, Germany).
20. ATP determination kit (Molecular Probes, Eugene, OR).
21. ApoGlow kit (Lumitech, Nottingham, UK).
22. Carboxy SNARF-1-acetoxymethyl ester acetate (SNARF-1, Molecular Probes, Eugene, OR) 23. DMSO (Sigma).
23. High K+ buffers of varying pH values (120 mM KCl, 30 mM NaCl, 0.5 mM $MgSO_4$, 1 mM $CaCl_2$, 1 mM $NaHPO_4$, 5 mM glucose and 10 mM HEPES).

24. Nigericin (Sigma, St. Louis, MO; diluted from a stock solution of 500 μg/ml in ethanol).
25. Deproteinizing buffer for glutathione (GSH) assay: 70 % perchloric acid and 15 mM bathophenanthrolinedisulfonic acid (BPDS, Sigma).
26. γ-Glutamyl glutamate (γ-Glu-Glu, Sigma), internal standard for GSH assay.
27. After repeated freezing and thawing, samples were centrifuged at 15,000×*g* for 3 min. 50 μl of 100 mM mono-iodo-acetic acid in 0.2 mM *m*-cresol purple was added to 500 μl supernatant. Samples were neutralized by addition of 480 μl of 2 M KOH and 2.4 M $KHCO_3$ and incubated in the dark at room temperature for 10 min. Then, 1 ml of 1 % fluoro-dinitrobenzene was added and the samples were incubated in the dark at 4 °C overnight. After centrifugation and filtering, 100 μl of supernatants were injected into the HPLC Model 2690 (Waters Alliance System, Milford, MA) equipped with a Model 996 photodiode array detector and Spherisorb NH_2 column (4.6×250 mm; 10 μm; Waters).
28. 7-Amino-4-trifluoromethyl-coumarin (AFC, Sigma).
29. Caspase substrate peptides: DEVD-AFC, Z-IETD-AFC, where Z represents a benzyloxycarbonyl group; caspase inhibitor peptides Z-Val-Ala-Asp(Ome).fmk (Z-VAD), Boc-Asp.fmk (Boc-Asp) as well as non-caspase cysteine protease inhibitor, Z-Phe-Ala.fmk (Z-FA) can be obtained from Enzyme Systems Products (Livermore, CA).
30. Caspase assay buffer: 250 mM sucrose, 20 mM HEPES–KOH pH 7.5, 50 mM KCl, 2.5 mM $MgCl_2$, 1 mM dithiothreitol.
31. Versene (Life Technologies).
32. Concanavalin A (Con A, Sigma).
33. Goat anti-mouse IgG (ICN, Aurora OH).
34. Tritiated thymidine, ^{3}HTdR (ICN).
35. CH-11 IgM monoclonal antibody to Fas/Apo-1/CD95 (Upstate Biotechnology, Saranac Lake, NY).
36. Complete RPMI medium: RPMI 1640 supplemented with 10 % fetal calf serum, 2 mM L-glutamine, 100 IU/ml penicillin, 100 μg/ml gentamicin, and 10 μg/ml amphotericin B.
37. Plastic tissue culture dishes (Becton Dickinson, Franklin Lake, NJ).
38. Phenol, chloroform, isoamyl alcohol, proteinase K, agarose (all RNase and DNase-free. molecular biology grade, from Sigma).
39. Spectrophotometer.

40. Luminometer.
41. Carbonyl cyanide *m*-chlorophenylhydrazone (mClCCP, Sigma).
42. Folin & Ciocalteu's Phenol Reagent Solution (Sigma).
43. 4 mm diameter 0.45 μm polypropylene filter (Whatman, Mainstead, England).
44. Monoclonal antibody to poly(ADP-ribose) polymerase (PARP) C-2-10 (53).
45. Monoclonal antibody 5F7 directed to C-terminal amino acids 176-460 of human FLICE/Mch5/caspase-8 (Panvera, Madison, WI).
46. Monoclonal antibody 31A1067 directed to caspase 3 (Gene Therapy Systems, San Diego, CA).
47. Monoclonal antibody C4 directed to human β actin (Boehringer, Indianapolis, IN).
48. Biotinylated secondary antibodies and horseradish peroxidase-conjugated avidin (Jackson Laboratories, West Grove, PA).
49. 4-Chloronaphthol (Sigma).
50. Enhanced chemiluminescence detection kit (Western Lightning Chemiluminescence Reagent Plus, PerkinElmer Life Sciences, Boston, MA).
51. Kodak Image Station 440CF equipped with Kodak 1D Image Analysis Software (Eastman Kodak Company, Rochester, NY).

3. Methods

The methods described below outline (1) in vitro lymphocyte culture, activation, and apoptosis assays, flow cytometric analysis of (2) $\Delta\psi_m$ and (3) ROI production and (4) intracellular pH, (5) measurement of intracellular ATP and ADP, (6) HPLC analysis of reduced (GSH) and oxidized forms of glutathione (GSSG), and (7) caspase enzyme assays (see Note 1).

3.1. Lymphocyte Culture, Activation, and Viability Assays

3.1.1. Separation of Peripheral Blood Mononuclear Cells

1. Collect peripheral blood in sterile tubes containing 50 U heparin (Sigma) per ml of blood.
2. Layer blood diluted 1:1 with PBS on Ficoll-Paque. Typically layer 10 ml diluted blood over 5 ml of Ficoll-Paque.
3. Centrifuge cells at 500×*g* for 30 min with centrifuge brake off.

4. Remove peripheral blood mononuclear cells (PBMC) from interface between Ficoll-Paque and plasma with pipettor.
5. Wash PBMC three times in PBS by centrifugation at 300 × *g* for 10 min.
6. PBMC are resuspended at 10^6 cells/ml in RPMI 1640 medium, supplemented with 10 % fetal calf serum, 2 mM L-glutamine, 100 IU/ml penicillin, and 100 μg/ml gentamicin (complete RPMI medium) and incubated for experiments at 37 °C in a humidified atmosphere with 5 % CO_2.

3.1.2. Separation of Monocytes and Peripheral Blood Lymphocytes

1. Precoat Petri dishes with autologous serum for 30 min at 37 °C.
2. Add 5 ml of PBMC (maximum 5×10^6/ml) to serum-pretreated dishes and incubate for 1 h at 37 °C.
3. Remove nonadherent cells by washing three times with 5 ml of warm (37 °C) complete RPMI medium.
4. To obtain a monocyte-enriched cell fraction wash dishes vigorously with warm medium.
5. Add 4 ml of ice-cold 0.05 % Versene and 1 ml autologous serum to each dish for 15 min at room temperature.
6. Scrape off loosely adherent monocytes with a rubber policeman under inverse microscopic control.
7. The monocyte-depleted fraction of peripheral blood lymphocytes (PBL) should contain less than 2 % monocytes, while the monocyte-enriched fraction should contain 90–95 % monocytes by staining with CD14 monoclonal antibody.

3.1.3. Cell Culture, Activation, and Viability Assays

Human PBL undergo apoptosis in response to repetitive activation through the T cell receptor, i.e., CD3/CD28 co-stimulation resulting in activation-induced cell death (AICD) (36, 37), cross-linking of cell surface death receptors such as Fas/Apo-1/CD95 (15) or elevation of intracellular ROI levels after treatment with H_2O_2 (24, 36). Monocytes/macrophages remove apoptotic bodies via phagocytosis, therefore processing of cell death signals by lymphocytes is best evaluated using PBL (see Note 2).

CD3/CD28 Co-stimulation of PBL

1. Precoat 10 cm diameter plastic Petri dishes with 100 μg/ml goat anti-mouse IgG (diluted in PBS) for 2 h at 37 °C.
2. Wash plates with PBS, add OKT3 monoclonal antibody (1 μg/ml), and incubate for 1 h at 37 °C.
3. Add PBL (10^6 cells/ml in complete RPMI medium).
4. For CD28 co-stimulation add 500 ng/ml mAb CD28.2 and incubate cells at 37 °C for the desired period of time.

Triggering Fas-Mediated Cell Death of PBL

1. Sensitize peripheral blood T cells for Fas-mediated apoptosis by CD3/CD28 co-stimulation or treatment with 5 μg/ml Con A for 5–7 days.
2. Monitor blast transformation by measurement of increased side scatter (SSC) using flow cytometry (16) or ^{3}HTdR incorporation via pulse-labeling with 0.4 μCi of ^{3}HTdR of 10^{5} cells in 100 μl per well of a 96-well plate (54).
3. Determine cell viability by staining with 0.25 % trypan blue in 0.9 % NaCl. Viable cells should not stain with trypan blue.
4. Pellet and resuspend cells at 2×10^{6} cells/ml in complete RPMI medium.
5. Add an equal volume of complete RPMI medium without (control) or with 2 μg/ml of CH11 IgM monoclonal antibody.
6. Incubate cells at 37 °C for the desired period of time.

Treatment with H_2O_2

1. Prepare fresh 10 mM H_2O_2 in PBS from 30 % stock solution.
2. Seed PBL at 2×10^{6} cells/ml in complete RPMI medium.
3. Add an equal volume of complete RPMI medium without (control) or with 100 μM H_2O_2.
4. Incubate cells at 37 °C for the desired period of time.

Monitoring of Cell Death

Apoptosis is monitored by observing cell shrinkage while counting trypan blue-stained cells, DNA fragmentation using agarose gel electrophoresis and quantified by flow cytometry after concurrent staining with fluorescein-conjugated annexin V (annexin V-FITC, R&D Systems, Minneapolis, MN; FL-1) and propidium iodide (PI, FL-2) as earlier described (14, 15, 55, 56). Staining with phycoerythrin-conjugated annexin V (annexin V-PE, R&D Systems) was used to monitor PS externalization (FL-2) in parallel with measurement of ROI levels and $\Delta\psi_m$ (see below). Apoptosis rates are expressed as percentage of annexin V-positive/PI-negative cells. Necrosis is assessed by observing cellular and nuclear swelling. Swollen nuclei of necrotic cells can be observed by staining with propidium iodide (PI, 50 μg/ml). Necrotic cells are enumerated by direct PI staining using flow cytometry and fluorescence microscopy. Necrosis rates are expressed as percentage of PI-positive population within annexin-positive cells (36) (see Note 4).

DNA Fragmentation Assay

1. Wash cells 3× in PBS using screw-capped 15 ml polypropylene tubes.
2. Resuspend up to 5×10^{7} cells in 100 mM NaCl, 10 mM Tris–HCL pH 8.0, and 1 mM EDTA.
3. Add 250 μl of 10 % SDS.

4. Add 200 μg/ml proteinase K (keep 5 mg/ml aliquots at –20 °C).
5. Incubate overnight at 37 °C.
6. Extract 2× with equal volume of phenol. Remove aqueous phase only. Do not remove interface.
7. Extract 2× with equal volume of chloroform:isoamylalcohol (24:1).
8. Precipitate DNA from aqueous phase with two volumes of absolute ethanol for 10 min at room temperature.
9. Transfer DNA with Pasteur pipette to 500 μl of TE in Eppendorf tube and let it dissolve for 30 min.
10. Add 1/10 volume of 3 M Na-acetate.
11. Add two volumes of absolute ethanol.
12. Precipitate DNA for 10 min at room temperature.
13. Repeat steps 9–12.
14. Dissolve DNA in 500 μl of 10 mM Tris–HCL pH 8.0 and 1 mM EDTA.
15. Quantify DNA by reading optical density at 260 nm (OD260). Read OD at 280 nm as well. OD260/280 should be 1.8–2.0. 1 OD corresponds to a DNA concentration of 50 μg/ml.
16. Store DNA at 4 °C until analysis in a 2 % agarose gel (14).

Assessment of Apoptosis and Necrosis by Flow Cytometry

1. Resuspend 2×10^5 cells to be analyzed in 200 μl of annexin binding buffer.
2. Add 5 μl of Annexin V-FITC (10 μg/ml) and 5 μl of PI (50 μg/ml).
3. Incubate cells at room temperature in the dark.
4. Analyze by flow cytometry by electronic gating on live cells based on forward scatter (FSC) and side scatter (SSC) and measuring Annexin-FITC binding on the FL1 channel (emission at 530 nm) and PI staining on the FL-2 channel (emission at 625 nm).

3.2. Flow Cytometric Analysis of the Mitochondrial Transmembrane Potential

Mitochondrial transmembrane potential ($\Delta\psi_m$) can be estimated by cationic lipophilic dyes with high binding affinity to the negatively charged inner mitochondrial membrane (9, 57, 58). Since binding characteristics do not completely overlap, parallel staining with several dyes is recommended (see Note 5).

1. Resuspend 2×10^5 cells in 200 μl of annexin binding buffer if concurrently stained with Annexin V-FITC or Annexin V-PE matching a potentiometric dye emitting FL-2 or FL-1 fluorescence, respectively. Alternatively, 2×10^5 cells can be

resuspended in 200 µl 5 mM HEPES-buffered saline (HBS containing 0.9 % NaCl pH 7.4). This buffer, lacking Ca^{2+}, does not allow concurrent staining with Annexin V.

2. Aliquots of cell suspensions are stained with several potentiometric dyes in parallel.
   (a) Add 200 µl of dye solution containing 20 nm $DiOC_6$ (excitation: 488 nm, emission: 525 nm recorded in FL-1). This dye can be added in combination with Annexin V-PE emitting FL-2 fluorescence (see Note 3).
   (b) Add 200 µl of dye solution containing 1 µM TMRM (excitation: 549 nm, emission: 573 nm recorded in FL-2). This dye can be added in combination with Annexin V-FITC emitting FL-1 fluorescence.
   (c) Add 200 µl of dye solution containing 0.5 µM JC-1. JC-1 selectively incorporates into mitochondria, where it forms monomers (fluorescence in green, 527 nm) or aggregates, at high transmembrane potentials (fluorescence in red, 590 nm) (59, 60).
3. Parallel cell suspensions should be treated 5 µM mClCCP. Co-treatment with this protonophore for 15 min at 37 °C results in decreased $DiOC_6$, TMRM, and JC-1 fluorescence and serves as a positive control for disruption of mitochondrial transmembrane potential (15).
4. Incubate cells in the dark for 15 min at 37 °C before flow cytometry.
5. For each sample, measurements are carried out on 10,000 cells.

3.3. Measurement of ROI Production

Production of ROI can be assessed fluorometrically using oxidation-sensitive fluorescent probes 5,6-carboxy-2′,7′-dichlorofluorescein-diacetate (DCFH-DA), dihydrorhodamine 123 (DHR), and hydroethidine (HE, Molecular Probes, Eugene, OR) as earlier described (14). Cells are stained in annexin binding buffer or HBS (see *Specific Protocol* below) with 0.1 µM DHR for 2 min, 1 µM DCFH-DA for 15 min, or 1 µM HE for 15 min and samples are analyzed using a Becton Dickinson FACStar Plus flow cytometer equipped with an argon ion laser delivering 200 mW of power at 488 nm. Fluorescence emission from 5,6-carboxy-2′,7′-dichlorofluorescein (DCF; green) or DHR (green) is detected at a wavelength of 530 ± 30 nm. Fluorescence emission from oxidized HE, ethidium (red), was detected at a wavelength of 605 nm. Dead cells and debris are excluded from the analysis by electronic gating on FSC and SSC measurements. While R123, the fluorescent product of DHR oxidation, binds selectively to the inner mitochondrial membrane, ethidium and DCF remain in the cytosol of living cells (61), thus, allowing measurement of ROI levels in different subcellular compartments.

Specific Protocol

1. Following apoptosis assay, wash cells two times in 5 mM HEPES-buffered saline (HBS, containing 0.9 % NaCl) pH 7.4.
2. Resuspend 2×10^5 cells in 200 μl of annexin binding buffer if concurrently stained with Annexin V-FITC or Annexin V-PE matching oxidation-sensitive dyes emitting FL-2 (HE) or FL-1 fluorescence (DCF, R123), respectively. Alternatively, 2×10^5 cells can be resuspended in 200 μl of 5 mM HBS. This buffer, lacking Ca^{2+}, does not allow concurrent staining with Annexin V.
3. Subsequently, aliquots of cell suspensions are stained with several potentiometric dyes in parallel.
   (a) Add 200 μl of dye solution containing 0.1 μM DHR (excitation: 488 nm, emission: 530 nm recorded in FL-1). This dye can be added in combination with Annexin V-PE emitting FL-2 fluorescence. Staining is done in the dark at room temperature for 2 min, timed with a stopwatch, followed by running on the flow cytometer.
   (b) Add 200 μl of dye solution containing 1 μM DCFH-DA (excitation: 488 nm, emission: 525 nm recorded in FL-1). This dye can be added in combination with Annexin V-PE emitting FL-2 fluorescence. Staining is done in the dark at room temperature for 15 min, timed with a stopwatch, followed by running on the flow cytometer.
   (c) Add 200 μl of dye solution containing 1 μM HE (excitation: 488 nm, emission: 605 nm recorded in FL-2). This dye can be added in combination with Annexin V-FITC emitting FL-1 fluorescence. Staining is done in the dark at room temperature for 15 min, timed with a stopwatch, followed by running on the flow cytometer.
4. For each sample, measurements are carried out on 10,000 cells.

3.4. Intracellular pH Measurement

Intracellular pH measurements are carried out with flow cytometry using the pH-sensitive dye carboxy SNARF-1-acetoxymethyl ester acetate (SNARF-1) as described by Wieder et al. (62). SNARF-1 enters cells passively as a nonpolar ester. It is then hydrolyzed by intracellular esterases into a polar compound unable to leave membrane-intact cells. The emission spectrum of SNARF-1 undergoes a pH-dependent wavelength shift. The ratio of fluorescence intensities emitted at two different wavelengths (FL2:580 nm and FL3:650 nm) is used for determination of pH.

1. Make fresh 0.5 mg/ml stock solutions of SNARF-1 daily in DMSO.
2. Resuspend 5×10^5 cells in 500 µl of PBS.
3. Add 5 µg/ml SNARF-1 to the cells and incubate samples 30 min at 37 °C.
4. Wash cells once in 1 ml of PBS and resuspend in 500 µl of PBS.
5. Analyze on a Becton Dickinson FACStar Plus flow cytometer. The SNARF-1 dye is excited with 200 mW of the 488 nm argon laser and fluorescence is collected in two wavelengths (FL2:580 nm and FL3:650 nm) in the pulse processing mode.
6. Generate a standard calibration curve for each experiment by staining the cells in high K+ buffers of varying pH values (120 mM KCl, 30 mM NaCl, 0.5 mM $MgSO_4$, 1 mM $CaCl_2$, 1 mM $NaHPO_4$, 5 mM glucose and 10 mM HEPES) in the presence of 5 µg/ml nigericin to equilibrate the intracellular/extracellular pH.
7. Calculate intracellular pH based on FL3/FL2 ratio.

3.5. Measurement of Intracellular ATP and ADP Levels

T cell activation and apoptosis require the energy provided by ATP (63). Intracellular ATP concentration is a key switch in the cell's decision to die via apoptosis or necrosis (64) and, therefore, depletion of ATP may be responsible for defective apoptosis and a predisposition to necrosis in patients with SLE (36). Intracellular ATP levels can be determined with great sensitivity and specificity using the luciferin–luciferase method (65). Addition of luciferin and firefly luciferase to ATP-containing biological sample results in light emission. The luminometric ATP assay is based on the firefly luciferase reaction:

$$\text{ATP} + \text{D-Luciferin} + \text{O}_2 \rightarrow \text{AMP} + \text{pyrophosphate} + \text{oxyluciferin} + \text{CO}_2 + \text{light}.$$

The quantum efficiency is very high resulting in almost one photon per ATP molecule consumed in the reaction. The light is measured in luminometer. Under assay conditions of constant luciferase activity, intensity of the emitted light is proportional to the ATP concentration. The assay is calibrated by the addition of a known amount of ATP.

3.5.1. Collection of Cells for ATP Assay

1. Collect 5×10^6 PBL by centrifugation at $300 \times g$ for 10 min and wash once in PBS.
2. Resuspend cell pellet in 50 µl of PBS and mix with equal volumes of 2.5 % trichloroacetic acid. Such extracts can be stored at −20 °C.
3. Measure the total protein content of each sample using the Lowry assay (66).

3.5.2. Lowry Assay

Stock Solutions

Lowry A: 2 % Na_2CO_3 in 0.1 M NaOH.
Lowry B: 1 % $CuSO_4$ in diH_2O.
Lowry C: 2 % sodium potassium tartrate ($NaKC_4H_4O_6{\cdot}4H_2O$).

Reagents

Lowry Stock Reagent

49 ml Lowry A.
0.5 ml Lowry B and 0.5 ml Lowry C.

Folin's Reagent: Phenol reagent—2N (Folin-Ciocalteau reagent). Dilute 1:1 in diH_2O before use. BSA standard solution is prepared as described in Table 2. The standard calibration solution is dissolved at a concentration of 1 mg/ml in a buffer similar to the biological sample of unknown protein content, such as PBS.

Assay Procedure

1. Add 100 µl of sample (sample + buffer = 100 µl) per tube.
2. Add 1.0 ml of Lowry stock reagent to each tube.
3. Incubate 30 min at room temperature.
4. Add 100 ml of Folin's reagent to each tube.
5. Incubate 30 min at room temperature.
6. Read in a spectrophotometer at 595 nm.

3.5.3. ATP Assay

The ATP contents of PBLs from patients with SLE and control donors were assayed in parallel.

The bioluminescence assay was performed using an ATP determination kit (A22066, Invitrogen, Carslbad, CA) according to the manufacturer's instructions. Utilizing a Synergy 2 Multi-Mode Microplate Reader (BioTek, Winooski, VT), equipped with automatic reagent dispensers; in all-white, flat-bottom, 96-well plates (Cat. No 7571, Thermo Scientific, Rochester, NY), ATP standard

Table 2
Preparation of protein standard solution for Lowry assay

Standard solution protein amount (µg)	Standard solution volume(µl)	Buffer volume (µl)
0	0	100
10	10	90
20	20	80
30	30	70
50	50	50
75	75	25
100	100	0

The standard calibration solution is dissolved at a concentration of 1 mg/ml in a buffer similar to the biological sample of unknown protein content, such as PBS

curves are established in each experiment and should be linear in the 5- to 5,000-nM range. In our laboratory, the sample volume added to the reaction mixtures was less than 5 % of the total assay volume (67). In our lab, the sample volume added to the reaction mixtures was less than 2 % of the total assay volume.

Precautions

Because of the high sensitivity of the luciferin–luciferase reaction, avoid contamination with ATP from exogenous biological sources, such as bacteria or fingerprints. Therefore, latex or vynil gloves are to be worn at all times.

Protect the D-luciferin and firefly luciferase reagents from light.

Mix solutions containing firefly luciferase *gently*, for example, by inversion; vortex mixing may denature the enzyme.

Arsenate compounds may inhibit the reaction.

The temperature optimum for the reaction is 28 °C. At higher temperatures, the reaction is slower.

Reagents

1. D-Luciferin (MW 302) 3 mg of lyophilized powder per vial.
2. Luciferase, firefly recombinant,40 μl of a 5 mg/ml solution in 25 mM Tris–HCL-acetate, pH 7.8, 0.2 M ammonium sulfate, 15 % (v/v) glycerol and 30 % (v/v) ethylene glycol.
3. Dithiothreitol (DTT) (MW 154) 25 mg.
4. Adenosine 5′-triphosphate (ATP), 400 μl of a 5 mM solution in TE buffer.
5. 20× Reaction Buffer, 10 ml of 500 mM Tricine buffer, pH 7.8, 100 mM $MgSO_4$, 2 mM EDTA, and 2 mM sodium azide.
6. Standard reaction solution containing 0.5 mM D-luciferin, 1.25 μg/ml firefly luciferase, 25 mM Tricine buffer, pH 7.8, 5 mM $MgSO_4$, 100 μM EDTA and 1 mM DTT.

Store reagent frozen at –80 °C. Avoid repeated freezing and thawing.

ATP Assay Protocol

1. Make 1.0 ml of 1× Reaction Buffer by adding 50 μl of 20× Reaction Buffer to 950 μl of deionized autoclaved H_2O. This volume will be sufficient to make 1 ml of 10 mM D-luciferin stock solution.
2. Make 1 ml of a 10 mM D-luciferin stock solution by adding 1 ml of 1× Reaction Buffer (prepared in step 1 in "ATP Assay Protocol") to one vial of D-luciferin (3 mg of lyophilized powder). Protect from light until use. The D-luciferin stock solution is reasonably stable for several weeks if stored at –20 °C, protected from light.
3. Prepare a 100 mM DTT stock solution by adding 1.62 ml of H_2O to 25 mg of DTT. Aliquot into ten 160 μl volumes and

store frozen at –20 °C. Stock solutions of DTT stored properly are stable for 6 months to 1 year. Thawed aliquots should be kept on ice until ready for use.

4. Prepare low-concentration ATP standard solutions from 5 nM to 5 μM by diluting the 5 mM ATP stock solution in H_2O. These dilute solutions are stable for several weeks when stored at –20 °C.
5. Make 10 ml of a standard reaction solution by combining the following:

   8.9 ml dH_2O.

   0.5 ml 20× Reaction Buffer.

   0.1 ml 0.1 M DTT.

   0.5 ml of 10 mM D-luciferin.

   2.5 μl of firefly luciferase 5 mg/ml stock solution.
6. Gently mix the tube by inverting THREE times. The firefly luciferase enzyme is easily denatured by vortexing. Keep the reaction solution protected from light until use.
7. Create standard curve.
   (a) Measure luminescence of standard reaction solution (prepared in step 5 in Subheading "ATP Assay Protocol") which is considered as background.
   (b) Start the reaction by adding the desired amount of dilute ATP standard solution (prepared in step 4 in Subheading "ATP Assay Protocol") and read the luminescence. The volume of the dilute ATP standard solution that is added to the standard assay solution should be no more than 10 %, preferably less than 2 %, of the total assay volume.
   (c) Subtract the background luminescence.
   (d) Generate a standard curve for a series of ATP concentrations. Be sure to always add a constant sample volume of the ATP-containing solution as internal standard.
8. Sample Analysis
   (a) Add experimental sample to standard reaction solution. The total volume of the experimental sample assays should be equal to that of the ATP standard assays, with the amount of experimental sample added no more than 10 % of the total assay volume.
   (b) Calculate the amount of ATP in the experimental samples from the standard curve.

Assessment of ATP/ADP Ratio and ADP Levels

ADP can be measured by its conversion to ATP, using the ApoGlow kit (Lumitech, Nottingham, UK). The produced ATP is then detected by the above luciferin–luciferase method.

1. Dispense 100 µl of standard reaction solution with experimental sample as described in step 8a in "ATP Assay Protocol" into 96 well plates.
2. Load plate into 96-well plate reader and record luminescence: reading A.
3. After 10 min lag period, add 20 µl of ADP-converting reagent to each well using multichannel pipettor or autodispenser built into luminometer if available.
4. Take a 1 s integrated reading: reading B. If autoinjector is unavailable, reading B should be taken before addition of ADP-converting reagent.
5. After 5 min incubation allowing conversion of ADP to ATP take a final 1 s integrated reading: reading C.
6. ADP:ATP ratio is calculated as follows: $(C-B)/A$.

3.6. HPLC Assay of Glutathione Levels

Reduced (GSH) and oxidized glutathione (GSSG) as well as other intermediates of GSH metabolism can be concurrently measured by reverse phase ion-exchange high-performance liquid chromatography (HPLC) using UV detection at 365 nm (68).

We use a two-step derivatization procedure: (1) *S*-carboxymethylation of the reduced SH groups with iodoacetic acid to prevent their oxidation and (2) *N*-dinitrophenylation with 1-fluoro,2,4-dinitrobenzene to allow UV detection (Fig. 2).

1. Wash 2×10^7 PBL once in 5 ml of PBS and store cell pellet at −80 °C until assay.
2. Resuspend cell pellet in 250 µl of H_2O. Use 10 µl of cell suspension to measure protein content as described in Subheading 3.5.2.
3. Add 50 µl of 70 % perchloric acid, 25 µl of 15 mM BPDS to deproteinize sample as well as 25 µl of γ-Glu-Glu as internal standard.

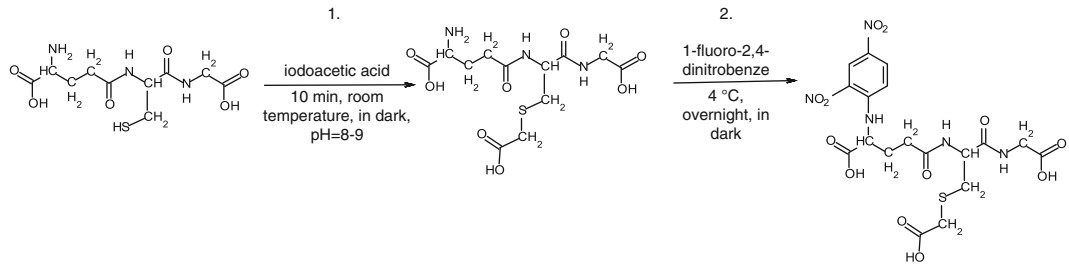

Fig. 2. The two-step derivatization of GSH.

4. Vortex, freeze, and thaw the sample in two cycles.
5. Pellet sample in microcentrifuge at 15,000×*g* for 5 min and save supernatant.
6. Add 25 μl of 100 mM mono-iodo-acetic acid in 0.2 mM *m*-cresol purple to 250 μl of supernatant.
7. Adjust pH of acidic solution (pink in color) to pH 8–9 (purple in color) by addition of 240 μl of 2 M KOH and 2.4 M $KHCO_{3.}$
8. Incubate sample in the dark at room temperature for 10 min.
9. Add 1 ml of 1 % fluoro-dinitro-benzene, vortex, and incubate the samples in the dark at 4 °C overnight.
10. Centrifuge sample at 15,000×*g* for 10 min at 4 °C.
11. Filter supernatant through 4 mm diameter 0.45 μm polypropylene filter (Whatman, Maidstone, England).
12. Inject 50 μl of each sample into HPLC equipped with a Model 996 photodiode array detector (Waters Alliance System, Milford, MA) and a Waters Spherisorb 3-NH_2-propyl column (4.6×250 mm; 10 μm). A UV detector set to a wavelength of 365 nm can also be utilized.
13. After sample injection, a mobile phase of HPLC comprised of 80 % of Mobile Phase Solution A (80 % methanol) and 20 % of Mobile Phase Solution B (0.5 M sodium acetate dissolved in 64 % methanol) is maintained for 5 min, followed by a 10-min linear gradient to 1 % Mobile Phase Solution A/99 % Mobile Phase Solution B at a flow rate of 1.5 ml/min. Then, the mobile phase is held at 99 % Mobile Phase Solution B until the final compound, usually GSSG, has eluted (5–10 min).

3.7. Caspase Enzyme Assays

Activation of the caspase enzyme cascade is a hallmark of apoptosis. Caspase-3 is a key effector of all apoptosis pathways, amplifying the signal from initiator caspases (such as caspase-8) and indicating a final commitment to cellular disassembly. In addition to cleaving other caspases in the enzyme cascade, caspase-3 has been shown to cleave poly(ADP-ribose) polymerase (PARP), DNA-dependent protein kinase, protein kinase C, the 70 kDa component of U1 snRNP, and actin (see Note 6).

1. Induce apoptosis in cells by desired method. Remember to incubate a concurrent control culture without induction. Include cells treated with caspase inhibitor DEVD-CHO as negative control (15).
2. After washing cells once in PBS, pellet 10^6 cells per experimental sample at 400×*g* for 5 min. Cell pellet can be stored at –80 °C until measurement.

3. Resuspend cell pellet in 25 µl of chilled cell lysis buffer comprised of 10 mM HEPES/KOH (pH 7.4), 2 mM EDTA, 0.1 % CHAPS, 5 mM dithiothreitol, 1 mM phenylmethylsulphonylfluoride, 10 µg/ml pepstatin A, 20 µg/ml leupeptin, 10 µg/ml aprotinin. Alternatively, cell lysis buffer from Clontech can be used.
4. Incubate cell lysate on ice for 15 min.
5. Pellet cell lysates in a microcentrifuge at 15,000 × *g* for 10 min at 4 °C.

   Transfer the supernatants to new microcentrifuge tubes. Samples may be assayed immediately or frozen at -80 °C until measurement.
6. Add 25 µl of 2× reaction buffer containing 80 µM zDEVD-AFC substrate (derived from 1 mM stock in DMSO), 250 mM sucrose, 20 mM HEPES–KOH (pH 7.5), 50 mM KCl, 2.5 mM MgCl, 1 mM freshly added DTT. Set up parallel samples lacking zDEVD-AFC substrate and containing caspase 3 inhibitor peptide zDEVD-AFC.
7. Incubate at 37 °C for 15–60 min (depending on caspase activity) and add ice-cold H_2O to 1 ml. Reaction can be stored frozen at –80 °C for later measurement.
8. Prepare 12-point calibration curve with 0.002–4 µM AFC.
9. Read fluorescence of experimental samples with 400 nm excitation filter and 505 nm emission filter.
10. After reading the fluorescence take 0.4 ml aliquot from experimental samples and add 0.4 ml Lowry reagent and 0.2 ml Folin reagent (according to Lowry protocol described in Subheading 3.5.2) to measure protein content. Add lysis and reaction buffer to set up standard blank tubes.
11. Express caspase activity as pmoles AFC/min/mg protein. Activities vary between 1,000 and 5,000 U/mg protein.
12. Western blot analysis of caspase activity.

    Caspases are activated through proteolysis that can be monitored by Western blot analysis.

    (a) For visualization of poly(ADP-ribose) polymerase (PARP) caspase 3 and caspase 8, lyse 2×10^6 cells in 100 µl of 62.5 mM Tris–HCl pH 6.8, 6 M urea, 10 % glycerol, 2 % SDS, 0.00125 % bromophenol blue, and 5 % β-mercaptoethanol.

    (b) Sonicate lysate for 15 s, boil for 5 min, and store at –80 °C. (53).

    (c) Assess protein concentration by Lowry method (see Subheading 3.5.2).

(d) Separate 40 μg of total cell lysate in 10 μl per well by SDS-PAGE and electroblot to nitrocellulose (69).

(e) Incubate nitrocellulose strips in 100 mM Tris–HCL pH 7.5, 0.9 % NaCl, 0.1 % Tween 20, and 5 % skim milk with the primary antibodies, anti-PARP monoclonal antibody C-2-10 (53), anti-caspase 3 (GTS), anti-caspase-8 (Panvera), or actin mAb C4 (Boehringer, Indianapolis, IN) at a 1,000-fold dilution at room temperature overnight.

(f) After washing, incubate blots with biotinylated secondary antibodies, and, subsequently, with horseradish peroxidase-conjugated avidin. In between incubations the strips are vigorously washed in 0.1 % Tween-20, 100 mM Tris–HCL pH 7.5, and 0.9 % NaCl.

(g) The blots can be developed with a substrate comprised of 1 mg/ml 4-chloronaphthol and 0.003 % hydrogen peroxide or using enhanced chemiluminescence (ECL) detection.

(h) Activation of the caspase cascade is monitored by cleavage of caspase 3 (32 kDa precursor into 17 kDa active form), caspase 8 (55 kDa precursor into 42 kDa active doublet), and PARP (116 kDa precursor into 85 kDa fragment).

3.8. Measurement of Mitochondrial Electron Transport Chain Activity

The method described here explains (a) how to permeabilize PBL (70); (b) and measure the activity of the mitochondrial ETC (71, 72).

3.8.1. Reagents

1. Mannitol (Sigma).
2. KCl (Fisher).
3. MgCl (J.T. Baker, Phillipsburg, NJ).
4. K_2PO_4 (USB).
5. Digitonin (Sigma).
6. Bovine serum albumin fraction V, heat shock, fatty-acid free (BSA; Roche).
7. ADP (Sigma).
8. Sodium pyruvate (Sigma).
9. Malic acid (Sigma).
10. Rotenone (Sigma).
11. Succinic acid (Fisher).
12. ATP (Sigma).
13. Antimycin A (Sigma).
14. L-Ascorbic acid (Sigma).
15. *N*,*N*,*N*′,*N*′-Tetramethyl-*p*-phenylenediamine (TMPD; Sigma).
16. Oxygraph system (Hansatech Instruments, Norfolk, England).

3.8.2. Permeabilizing PBL

1. Wash PBL in PBS twice this is to ensure the cells are as clean as possible if they are not truly clean it can affect how well the cells are permeabilized.
2. Resuspend at a concentration of 5×10^6/ml in respiration buffer (RB) containing 0.3 M mannitol, 10 mM KCl, 5 mM MgCl, 10 mM K_2PO_4 pH adjusted to 7.4.
3. Set aside 300 μl of the cell suspension for whole cell respiration to determine the baseline respiration rate of your cells.
4. Add digitonin to a final concentration of 60 μg/ml, as an example, add 21 μl of a 2 mg/ml stock solution to 700 μl of cell suspension; digitonin purification is described in 3.9.4.
5. Incubate for 1 min at room temperature.
6. Add 5 volumes (e.g., 5×21 μl = 105 μl, for 700 μl of cell suspension) of RB containing 1 mg/ml of BSA (made fresh that day) to stop the permeablization of the cell membranes.
7. Spin down cells at $500 \times g$ for 10 min.
8. Resuspend the pellet at 5×10^6 cells/ml in RB containing 1 mg/ml BSA and 0.5 mM ADP (made fresh that day).
9. Let the cells rest at room temperature for 5 min.

3.8.3. Testing ETC Complexes I–IV

O_2 consumption is measured in a Hansatech Instruments Oxygraph system which uses of a Clark type polarographic sensor. A water bath is used to maintain the temperature in the chamber at 37 °C. The electrode disc is stored in a desecrator under vacuum when not in use, and is prepared prior to each use. Cleaning of the electrode is done when deemed necessary (see Notes 7–10).

Testing Complex I

(a) Place 300 μl of cell suspension into the oxygraph chamber.
(b) Collect a baseline reading.
(c) Add pyruvate and malate to final concentrations of 8 mM and 0.2 mM, respectively, to measure complex I activity.

Testing Complexes II–IV (If Possible Done in Separate Chamber)

(a) Inhibit complex I by adding Rotenone to a final concentration of 3 μM.
(b) Complex II is measured with the addition of 10 mM final concentration succinate and 130 μM ATP.
(c) Inhibit complex II with a final concentration of 1 μM antimycin A.
(d) Complexes III and IV are measured through the addition of ascorbate and TMPD to final concentrations of 10 and 0.2 mM respectively.

3.8.4. Digitonin Purification

1. Weigh an empty Eppendorf tube.
2. Add 40–50 mg of digitonin.

3. Add 1 ml of pure ethanol; the digitonin will not dissolve; however, this step will remove most impurities. Some batches of digitonin may be only 70 % pure.
4. Spin at 14,000 × *g* for 10 s discard the supernatant.
5. Repeat steps 3 and 4 two more times.
6. Air-dry pellet, weighing every 5 min until you get two consistent weights.
7. Resuspend the digitonin in H_2O to a final concentration of 2 mg/ml.
8. Spin at 14,000 × *g* for 1 min to remove any final impurities.
9. Collect the supernatant, this is to be considered the pure digitonin.

4. Notes

1. When assessing T cell activation and apoptosis in PBL of patients with SLE, parallel processing of PBL from healthy and inflammatory disease, such as rheumatoid arthritis, control donors is essential. We typically establish values for normal donors, and process cells from two controls in parallel with cells from two patients. Whenever possible, we use freshly isolated cells. Alternatively, PBL frozen in complete RMPI 1640 medium with 7.5 % DMSO/30 % FCS can be utilized when viability of defrosted cells exceeds 98 % by trypan blue staining.
2. Testing of apoptosis by PBMC vs. PBL may reflect influence of phagocytic activity by monocytes/macrophages. Such comparative analysis should be supplemented by direct analysis of macrophage phagocytosis. However, phagocytosis depends on many factors, such as Fc receptor polymorphisms, release of macrophage-activating factors by T and B cells. Therefore, we routinely analyze PBL as effectors.
3. Fluorochromes are kept as highly concentrated (>10 mM) stock solutions in DMSO at −80 °C, unless indicated otherwise. SNARF-1 is kept aliquoted in powder form and reconstituted in DMSO on the day of assay.
4. PI directly stains necrotic cells. As earlier described (14, 73), live or apoptotic cells do not stain with PI and require permeabilization with 0.1 % Triton X-100. When using hydroethidine (HE, FL-2) for ROI measurement, cells are co-stained with fluorescein-conjugated annexin V (annexin V-FITC, R&D Systems, FL-1). Thus, annexin V-PE or annexin V-FITC are matched with emission spectra of potentiometric and oxidation-sensitive fluorescent probes. Staining with annexin V alone or in combination with

DHR or $DiOC_6$ was carried out in 10 mM HEPES pH 7.4, 140 mM NaCl, and 2.5 mM $CaCl_2$. Using three-color fluorescence, mitochondrial ROI levels, $\Delta\psi_m$, and PS externalization within T cell subsets can be concurrently analyzed by parallel staining with DHR or $DiOC_6$ (FL1), annexin V-PE (FL2), and Quantum Red/Cy5-conjugated monoclonal antibodies directed to CD3, CD4, CD8 (Sigma, St. Louis, MO; FL3), CD45RA, and CD45RO (Pharmingen). Quantum Red contains two covalently linked fluorochromes, PE and Cy5. PE absorbs light energy at 488 nm and emits at 670 nm, in the excitation range of Cy5 which acts as an acceptor dye. For fluorescence microscopy, cells were photographed using a Nikon Eclipse E800 camera (Nikon Corporation, Tokyo, Japan). Green and red fluorescent images were digitally superimposed using SPOT software (Diagnostic Instruments, Sterling Heights, MI).

5. Mitochondrial transmembrane potential ($\Delta\psi_m$) can be estimated by cationic lipophilic dyes with high binding affinity to the negatively charged inner mitochondrial membrane (9, 57, 58). Since binding characteristics do not completely overlap, parallel staining with several dyes is recommended.
6. The AFC calibration curve is very stable when measured on the same instrument and setting.

   The caspase assay is time- and protein-dependent when done with the suggested cell number and substrate concentration. Specificity of the enzymatic reaction was tested by using caspase-3 inhibitor DEVD-CHO and caspase-1/ICE inhibitor YVAD-CMK at a concentration range of 50–300 μM (74). Caspase 8 activity can be tested by using Z-IETD-AFC as substrate. Caspase inhibitors Z-Val-Ala-Asp(Ome).fmk (Z-VAD) and Boc-Asp.fmk (Boc-Asp) as well as non-caspase cysteine protease inhibitor, Z-Phe-Ala.fmk (Z-FA) were tested at concentrations of 20, 50, and 300 μM (75).
7. For permeabilization of cell membrane prior to mitochondrial O_2 consumption assay, add digitonin until 80 % of cells stain with trypan blue. Permeabilized state is indicated by trypan blue staining of the cytosol but not the nucleus of cells.
8. The Hansatech O_2 electrode is cleaned whenever the silver ring builds up as black oxidized film. This will cause spikes in the O_2 in the rate of consumption. It is important to not overclean the electrode as the cleaning solutions can damage the resin.
9. Keep substrates at 37 °C when running O_2 consumption experiments. This will reduce fluctuations in O_2 reading from the addition of the substrates to 37 °C chamber.
10. Rotenone can stick to the plastic of the Oxygraph chamber. To prevent inadvertent inhibition of complex I, it is suggested to use separate chambers or two separate Oxygraph systems to measure complexes I and complexes II–IV, respectively.

References

1. Elkon KB (1994) Apoptosis in SLE—too little or too much? [Review] [45 refs]. Clin Exp Rheumatol 12:553–559
2. Perl A, Banki K (1999) Molecular mimicry, altered apoptosis, and immunomodulation as mechanisms of viral pathogenesis in systemic lupus erythematosus. In: Kammer GM, Tsokos GC (eds) Lupus: molecular and cellular pathogenesis, 1st edn. Humana, Totowa, NJ, pp 43–64
3. Cohen JJ, Duke RC, Fadok VA, Sellins KS (1992) Apoptosis and programmed cell death in immunity. Annu Rev Immunol 10:267–293
4. Thompson CB (1995) Apoptosis in the pathogenesis and treatment of disease. Science 267:1456–1462
5. Emlen W, Niebur JA, Kadera R (1994) Accelerated in vitro apoptosis of lymphocytes from patients with systemic lupus erythematosus. J Immunol 152:3685–3692
6. Casciola-Rosen LA, Anhalt G, Rosen A (1994) Autoantigens targeted in systemic lupus erythematosus are clustered in two populations of surface structures on apoptotic keratinocytes. J Exp Med 179:1317–1330
7. Kovacs B, Vassilopoulos D, Vogelgesang SA, Tsokos GC (1996) Defective CD3-mediated cell death in activated T cells from patients with systemic lupus erythematosus: role of decreased intracellular TNF-alpha. Clin Immunol Immunopathol 81:293–302
8. Skulachev VP (1999) Mitochondrial physiology and pathology; concepts of programmed death of organelles, cells and organisms. Mol Aspects Med 20:139–140
9. Xiang J, Chao DT, Korsmeyer SJ (1996) BAX-induced cell death may not require interleukin 1β-converting enzyme-like proteases. Proc Natl Acad Sci U S A 93:14559–14563
10. Susin SA, Zamzami N, Castedo M, Daugas E, Wang H-G, Geley S et al (1997) The central executioner of apoptosis: multiple connections between protease activation and mitochondria in Fas/Apo-1/CD95- and ceramide-induced apoptosis. J Exp Med 186:25–37
11. Vander Heiden M, Chandel NS, Williamson EK, Schumaker PT, Thompson CB (1997) Bcl-X_L regulates the membrane potential and volume homeostasis of mitochondria. Cell 91:627–637
12. Constantini P, Chernyak BV, Petronilli V, Bernardi P (1996) Modulation of the mitochondrial permeability transition pore by pyridine nucleotides and dithiol oxidation at two separate sites. J Biol Chem 271:6746–6751
13. Mayes PA (1993) The pentose phosphate pathway & other pathways of hexose metabolism. In: Murray RK, Granner DK, Mayes PA, Rodwell VW (eds) Harper's biochemistry, 23rd edn. Appleton & Lange, Norwalk, CT, pp 201–211
14. Banki K, Hutter E, Colombo E, Gonchoroff NJ, Perl A (1996) Glutathione levels and sensitivity to apoptosis are regulated by changes in transaldolase expression. J Biol Chem 271:32994–33001
15. Banki K, Hutter E, Gonchoroff N, Perl A (1999) Elevation of mitochondrial transmembrane potential and reactive oxygen intermediate levels are early events and occur independently from activation of caspases in Fas signaling. J Immunol 162:1466–1479
16. Perl A, Gergely P Jr, Puskas F, Banki K (2002) Metabolic switches of T-cell activation and apoptosis. Antiox Redox Signal 4(5):427–443
17. Meier B, Radeke HH, Selle S, Younes M, Sies H, Resch K et al (1989) Human fibroblasts release reactive oxygen species in response to interleukin-1 or tumor necrosis factor-α. Biochem J 263:539–545
18. Hennet T, Richter C, Peterhans E (1993) Tumor necrosis factor-α induces superoxide anion generation in mitochondria of L929 cells. Biochem J 289:587–592
19. Schulze-Osthoff K, Krammer PH, Droge W (1994) Divergent signaling via APO-1/Fas and the TNFreceptor, two homologous molecules involved in physiological cell death. EMBO J 13:4587–4596
20. Gergely P, Nekam K, Lang I, Kalmar L, Gonzalez-Cabello R, Perl A (1984) Ketoconazole in vitro inhibits mitogen-induced blastogenesis, antibody-dependent cellular cytotoxicity, natural killer activity and random migration of human leukocytes. Immunopharmacology 7:167–170
21. Williams MS, Henkart PA (1996) Role of reactive oxygen intermediates in TCR-induced death of T cell blasts and hybridomas. J Immunol 157:2395–2402
22. Gulbins E, Brenner B, Schlottmann K, Welsch J, Heinle H, Koppenhoefer UL et al (1996) Fas-induced programmed cell death is mediated by a Ras-regulated O2-synthesis. Immunology 89:205–212
23. Um HD, Orenstein JM, Wahl SM (1996) Fas mediates apoptosis in human monocytes by a reactive oxygen intermediate dependent pathway. J Immunol 156:3469–3477
24. Puskas F, Gergely P, Banki K, Perl A (2000) Stimulation of the pentose phosphate pathway

and glutathione levels by dehydroascorbate, the oxidized form of vitamin C. FASEB J 14: 1352–1361

25. Li P-F, Dietz R, von Harsdorf R (1999) p53 regulates mitochondrial membrane potential through reactive oxygen species and induces cytochrome c-independent apoptosis blocked by bcl-2. EMBO J 18:6027–6036
26. Gottlieb E, Vander Heiden MG (2000) Thompson CB. Bcl-XL prevents the initial decrease in mitochondrial membrane potential and subsequent reactive oxygen species production during tumor necrosis factor alpha-induced apoptosis. Mol Cell Biol 20:5680–5689
27. Scarlett JL, Sheard PW, Hughes G, Ledgerwood EC, Ku H-H, Murphy MP (2000) Changes in mitochondrial membrane potential during staurosporin-induced apoptosis in Jurkat cells. FEBS Lett 475:267–272
28. Sanchez-Alcazar JA, Ault JG, Khodjakov A, Schneider E (2000) Increased mitochondrial cytochrome c levels and mitochondrial hyperpolarization precede camptothecin-induced apoptosis in Jurkat cells. Cell Death Differ 7(11):1090–1100
29. Almeida A, Almeida J, Bolanos JP, Moncada S (2001) Different responses of astrocytes and neurons to nitric oxide: the role of glycolytically generated ATP in astrocyte protection. Proc Natl Acad Sci U S A 98(26):15294–15299
30. Tewari M, Dixit VM (1995) Fas- and tumor necrosis factor-induced apoptosis is inhibited by the Poxvirus *crmA* gene product. J Biol Chem 270:3255–3260
31. Los M, Van de Craen M, Penning LS, Schenk H, Westendorp M, Baeuerle PA et al (1995) Requirement of an ICE/CED-3 protease for Fas/Apo-1-mediated apoptosis. Nature 375:81–83
32. Enari M, Hug H, Nagata S (1995) Involvement of an ICE-like protease in Fas-mediated apoptosis. Nature 375:78–81
33. Salvesen GS, Dixit VM (1997) Caspases: Intracellular signaling by proteolysis. Cell 91:443–446
34. Gross A, McDonnell JM, Korsmeyer SJ (1999) BCL-2 family members and the mitochondria in apoptosis [Review] [122 refs]. Genes Dev 13:1899–1911
35. Banki K, Hutter E, Gonchoroff NJ, Perl A (1998) Molecular ordering in HIV-induced apoptosis: oxidative stress, activation of caspases, and cell survival are regulated by transaldolase. J Biol Chem 273:11944–11953
36. Gergely PJ, Grossman C, Niland B, Puskas F, Neupane H, Allam F et al (2002) Mitochondrial hyperpolarization and ATP depletion in patients with systemic lupus erythematosus. Arthritis Rheum 46:175–190
37. Gergely PJ, Niland B, Gonchoroff N, Pullmann R Jr, Phillips PE, Perl A (2002) Persistent mitochondrial hyperpolarization, increased reactive oxygen intermediate production, and cytoplasmic alkalinization characterize altered IL-10 signaling in patients with systemic lupus erythematosus. J Immunol 169:1092–1101
38. Stryer L (1988) Biochemistry, 3rd edn. W.H. Freeman and Company, New York
39. Nagy G, Koncz A, Perl A (2003) T cell activation-induced mitochondrial hyperpolarization is mediated by Ca^{2+}- and redox-dependent production of nitric oxide. J Immunol 171:5188–5197
40. Clementi E, Brown GC, Feelisch M, Moncada S (1998) Persistent inhibition of cell respiration by nitric oxide: crucial role of S-nitrosylation of mitochondrial complex I and protective action of glutathione. Proc Natl Acad Sci U S A 95(13):7631–7636
41. Desai BN, Myers BR, Schreiber SL (2002) FKBP12-rapamycin-associated protein associates with mitochondria and senses osmotic stress via mitochondrial dysfunction. Proc Natl Acad Sci U S A 99:4319–4324
42. Fernandez D, Bonilla E, Mirza N, Perl A (2006) Rapamycin reduces disease activity and normalizes T-cell activation-induced calcium fluxing in patients with systemic lupus erythematosus. Arthritis Rheum 54(9):2983–2988
43. Fernandez DR, Telarico T, Bonilla E, Li Q, Banerjee S, Middleton FA et al (2009) Activation of mTOR controls the loss of TCRζ in lupus T cells through HRES-1/Rab4-regulated lysosomal degradation. J Immunol 182:2063–2073
44. Sen CK, Packer L (1996) Antioxidant and redox regulation of gene transcription [see comments]. [Review] [94 refs]. FASEB J 10:709–720
45. Li N, Karin N (1999) Is NF-kB the sensor of oxidative stress? FASEB J 13:1137–1143
46. Le Moine O, Louis H, Stordeur P, Collet JM, Goldman M, Deviere J (1997) Role of reactive oxygen intermediates in interleukin 10 release after cold liver ischemia and reperfusion in mice. Gastroenterology 113:1701–1706
47. Georgescu L, Vakkalanka RK, Elkon KB, Crow MK (1997) Interleukin-10 promotes activation-induced cell death of SLE lymphocytes mediated by Fas ligand. J Clin Invest 100:2622–2633
48. Suwannaroj S, Lagoo A, Keisler D, McMurray RW (2001) Antioxidants suppress mortality in

the female NZB × NZW F1 mouse model of systemic lupus erythematosus (SLE). Lupus 10(4):258–265

49. Demedts M, Behr J, Buhl R, Costabel U, Dekhuijzen R, Jansen HM et al (2005) High-dose acetylcysteine in idiopathic pulmonary fibrosis [see comment]. N Engl J Med 353:2229–2242
50. Nagy G, Barcza M, Gonchoroff N, Phillips PE, Perl A (2004) Nitric oxide-dependent mitochondrial biogenesis generates Ca2+ signaling profile of lupus T cells. J Immunol 173(6):3676–3683
51. Weinberg JB, Granger DL, Pisetsky DS, Seldin MF, Misukonis MA, Mason SN et al (1994) The role of nitric oxide in the pathogenesis of spontaneous murine autoimmune disease: Increased nitric oxide production and nitric oxide synthase expression in MRL-lpr/lpr mice, and reduction of spontaneous glomerulonephritis and arthritis by orally administered N^G-monomethyl-L-arginine. J Exp Med 179:651–660
52. Gilkeson GS, Mudgett JS, Seldin MF, Ruiz P, Alexander AA, Misukonis MA et al (1997) Clinical and serologic manifestations of autoimmune disease in MRL-lpr/lpr mice lacking nitric oxide synthase type 2. J Exp Med 186:365–373
53. Lamarre D, Talbot B, De Murcia G, LaPlante C, LeDuc Y, Mazen A et al (1988) Structural and functional analysis of poly(ADP-ribose) polymerase: an immunological study. Biochim Biophys Acta 950:147–160
54. Colombo E, Banki K, Tatum AH, Daucher J, Ferrante P, Murray RS et al (1997) Comparative analysis of antibody and cell-mediated autoimmunity to transaldolase and myelin basic protein in patients with multiple sclerosis. J Clin Invest 99:1238–1250
55. Vermes I, Haanen C, Steffens-Nakken H, Reutelingsperger C (1995) A novel assay for apoptosis. Flow cytometric detection of phosphatidylserine expression on early apoptotic cells using fluorescein labelled Annexin V. J Immunol Methods 184:39–51
56. Martin SJ, Reutelingsperger CPM, McGahon AJ, Rader JA, van Schie CAA, LaFace DM et al (1995) Early redistribution of plasma membrane phosphatidylserine is a general feature of apoptosis regardless of the initiating stimulus: inhibition by overexpression of bcl-2 and Abl. J Exp Med 182:1545–1556
57. Petit PX, O'Connor JE, Grunwald D, Brown SC (1990) Analysis of the membrane potential of rat- and mouse-liver mitochondria by flow cytometry and possible applications. Eur J Biochem 194:389–397
58. Tanner MK, Wellhausen SR, Klein JB (1993) Flow cytometric analysis of altered mononuclear cell transmembrane potential induced by cyclosporin. Cytometry 14:59–69
59. Smiley ST, Reers M, Mottola-Hartshorn C, Lin M, Chen A, Smith TW et al (1991) Intracellular heterogeneity in mitochondrial membrane potentials revealed by a J-aggregate-forming cation JC-1. Proc Natl Acad Sci U S A 88:3671–3675
60. Cossarizza A, Franceschi C, Monti D, Salvioli S, Bellesia E, Rivabene R et al (1995) Protective effect of N-acetylcysteine in tumor necrosis factor-α-induced apoptosis in U937 cells: The role of mitochondria. Exp Eye Res 220:232–240
61. Royall JA, Ischiropoulos H (1993) Evaluation of 2′,7′-dichlorofluorescein and dihydrorhodamine 123 as fluorescent probes for intracellular H_2O_2 in cultured endothelial cells. Arch Biochem Biophys 302:348–355
62. Wieder ED, Hang H, Fox MH (1993) Measurement of intracellular pH using flow cytometry with carboxy-SNARF-1. Cytometry 14:916–921
63. Fiers W, Beyaert R, Declercq W, Vandenabeele P (1999) More than one way to die: apoptosis, necrosis and reactive oxygen damage. Oncogene 18:7719–7730
64. Leist M, Single B, Castoldi AF, Kuhnle S, Nicotera P (1997) Intracellular adenosine triphosphate (ATP) concentration: a switch in the decision between apoptosis and necrosis. J Exp Med 185:1481–1486
65. Lundin A (2000) Use of firefly luciferase in ATP-related assays of biomass, enzymes, and metabolites. Methods Enzymol 305:346–370
66. Lowry OH, Rosebrough NJ, Farr AL, Randall RJ (1951) Protein measurement with the Folin phenol reagent. J Biol Chem 193:265–275
67. Lundin A (1994) ATP extractants neutralized by cyclodextrins. In: Campbell AK, Kricka LJ, Stanley PE (eds) Biolumimescence and chemiluminescence. Wiley, Chichester, pp 399–402
68. Fariss MW, Reed DJ (1987) High-performance liquid chromatography of thiols and disulfides: dinitrophenol derivatives. Methods Enzymol 143:101–109
69. Towbin HH, Staehelin T, Gordon J (1979) Electrophoretic transfer of proteins from polyacrylamide gels to nitrocellulose sheets: procedure and some applications. Proc Natl Acad Sci U S A 76:4350–4354
70. Rustin P, Parfait B, Chretien D, Bourgeron T, Djouadi F, Bastin J et al (1996) Fluxes of nicotinamide adenine dinucleotides through mitochondrial membranes in human cultured cells. J Biol Chem 271(25):14785–14790

71. Barrientos A (2002) In vivo and in organello assessment of OXPHOS activities. Methods 26(4):307–316
72. Rustin P, Chretien D, Bourgeron T, Gerard B, Rotig A, Saudubray JM et al (1994) Biochemical and molecular investigations in respiratory chain deficiencies. [Review] [25 refs]. Clin Chim Acta 228(1):35–51
73. Nicoletti I, Migliorati G, Pagliacci MC, Grignani F, Riccardi C (1991) A rapid and simple method for measuring thymocyte apoptosis by propidium iodide staining and flow cytometry. J Immunol Methods 139:271–279
74. Nicholson DW, Ali A, Thornberry NA, Vaillancourt JP, Ding CK, Gallant M et al (1995) Identification and inhibition of ICE/CED-3 protease necessary for mammalian apoptosis. Nature 376:37–43
75. Armstrong RC, Aja T, Xiang J, Gaur S, Krebs JF, Hoang K et al (1996) Fas-induced activation of the cell death-related protease CPP32 is inhibited by bcl-2 and by ICE family protease inhibitors. J Biol Chem 271:16850–16855
76. Lorenz HM, Grunke M, Hieronymus T, Herrmann M, Kuhnel A, Manger B (1997) In vitro apoptosis and expression of apoptosis-related molecules in lymphocytes from patients with systemic lupus erythematosus and other autoimmune diseases. Arthritis Rheum 40:306–317
77. Eisner MD, Amory J, Mullaney B, Tierney L Jr, Browner WS (1996) Necrotizing lymphadenitis associated with systemic lupus erythematosus. Semin Arthritis Rheum 26:477–482
78. Llorente L, Zou W, Levy Y, Richaud-Patin Y, Wijdenes J, Alcocer-Varela J et al (1995) Role of interleukin 10 in the B lymphocyte hyperactivity and autoantibody production of human systemic lupus erythematosus. J Exp Med 181:839–844
79. Green JM, Thompson CB (1994) Modulation of T cell proliferative response by accessory cell interactions [Review] [50 refs]. Immunol Res 13:234–243
80. Los M, Schenk H, Hexel K, Baeuerle PA, Droge W, Schulze-Osthoff K (1995) IL-2 gene expression and NF-kappa B activation through CD28 requires reactive oxygen production by 5-lipoxygenase. EMBO J 14:3731–3740
81. Tatla S, Woodhead V, Foreman JC, Chain BM (1999) The role of reactive oxygen species in triggering proliferation and IL-2 secretion in T cells. Free Radic Biol Med 26:14–24
82. Casciola-Rosen LA, Miller DK, Anhalt GJ, Rosen A (1994) Specific cleavage of the 70 kDa protein component of the U1 small nuclear ribonucleoprotein is a characteristic biochemical feature of apoptotic cell death. J Biol Chem 269:30757–30760
83. Perl A, Banki K (2000) Genetic and metabolic control of the mitochondrial transmembrane potential and reactive oxygen intermediate production in HIV disease. Antioxid Redox Signal 2:551–573
84. Puskas F, Gergely PJ, Niland B, Banki K, Perl A (2002) Differential regulation of hydrogen peroxide and Fas-dependent apoptosis pathways by dehydroascorbate, the oxidized form of vitamin C. Antioxid Redox Signal 4(3):358–369
85. Harada H, Becknell B, Wilm M, Mann M, Huang LJ, Taylor SS et al (1999) Phosphorylation and inactivation of BAD by mitochondria-anchored protein kinase A. Mol Cell 3:413–422
86. Nisoli E, Carruba MO (2006) Nitric oxide and mitochondrial biogenesis. J Cell Sci 119(14):2855–2862
87. Ibiza S, Victor VM, Bosca I, Ortega A, Urzainqui A, O'Connor JE et al (2006) Endothelial nitric oxide synthase regulates T cell receptor signaling at the immunological synapse. Immunity 24(6):753–765